05

Calibration of piezoelectric broadband field mine acoustic sensors and their practical application

© Kh.F. Makhmudov, V.N. Saveliev

Ioffe Institute,
194021 St. Petersburg, Russia
e-mail: h.machmoudov@mail.ioffe.ru

Received January 31, 2024
Revised November 16, 2024
Accepted December 25, 2024

An algorithm for optimizing the use of piezoelectric broadband sensors in the field has been developed. The amplitude of volumetric longitudinal waves from a reference source was measured in the laboratory to determine the sensitivity coefficient of piezoelectric broadband sensors. The possibility and expediency of using these sensors for practical purposes is considered. It has been established that they can be used in mining. By creating portable field equipment and adapting laboratory calibration methods, we have successfully diagnosed individual lines of a stationary acoustic emission automated monitoring system for underground structures in the field. An algorithm of actions is proposed and a method for adapting the developed laboratory techniques for mining operations with concrete reinforcement forming underground structures is substantiated.

Keywords: acoustic emission, monitoring, calibration, elastic wave.

DOI: 10.61011/TP.2025.04.61207.26-24

Introduction

Studying parameters of elastic waves in various objects makes it possible to evaluate mechanical stability and operational safety of large-scale underground structures including hazardous waste storages, tunnels and liquified gas reservoirs. These tasks are still relevant today and require continuous attention and development [1–4].

The main method of research includes registration and analysis of pulses of acoustic emission (AE), which is widely used for studying initial stages of the destruction process (nucleation and accumulation of microscopic cracks) in heterogeneous materials such as construction, structural and composite materials [5–9] and rocks [10–14]. When brittle heterogeneous bodies are mechanically loaded, damage is developed through a gradual accumulation of microcracks since such materials have many „weak points“, primarily in intergranular interlayers [14,15].

Propagation of an acoustic pulse (AP) in rocks and concretes with specified structural and mechanical characteristics is examined in detail in [16–18]. The applied procedure determines the velocity of AR propagation by the first arrival of the signal to a piezoelectric sensor of acoustic emission (AES) designed to record pulses in the broad band of frequencies. The measured AR velocity for the rock and the concrete layer agrees well with the calculations based on known formulae of the elasticity theory (taking into account the geometry of the layer in the latter case).

A shape of the acoustic wave from a reference source was controlled using the photoelasticity method [19], which has been used to determine a frequency range and calibrate special AESes designed to control excavations and to be installed in wells. Using a spectral analyzer, the energy balance has been calculated in the entire path „AR source–propagation medium–AR receiver“. A source of radiation of the acoustic wave was elastic collision of a steel ball with a sample surface (laboratory research) or a surface of the element of the underground structure (research in the field)

A series of methodical works [20,21] has been also performed in accordance with the requirement of [22] in order to evaluate capabilities of the developed algorithm for use in natural conditions of excavations. The research beginning included comparison of calculation results of coordinates of the AE sources for two different algorithms applied in the works [23–26]. It is known that accuracy of coordinate determination of the acoustic emission sources substantially depends on how accurately the velocity of a longitudinal wave is specified [27]. That is why it is desirable after installation of the sensors on the research object to scan across all the possible directions in order to specify a field of elastic wave velocities more exactly. It should be noted that the experiments [27–29] of loading rock samples have shown that the velocity field changes substantially during loading and, moreover, inhomogeneously in different directions. One of the possible reason for such velocity changing is opening or closing of the cracks oriented in any direction. In this regard, it is of a key importance to periodically determine the field of the velocities of elastic waves in various directions in a rock massive during its AE control in order to calculate the coordinates of the AR source.

Within the framework of the present work, the velocities have been determined for correct evaluation of results of acoustic emission monitoring of a complex underground structure with concrete reinforcement inside the rock massive.

1. Determination of frequency responses of the field piezoelectric acoustic emission sensors in the laboratory

The work has been performed by comparing the recorded signals from the piezoelectric film sensor (PFS) with the reference signals obtained by the photoelasticity method for the same conditions of field excitation of elastic oscillations in the reference sample. It was excited by collision of the steel ball of the diameter of 2.3 mm with a surface of the glass prism $190 \times 240 \times 240$ mm. The photoelasticity method is designed to record an undistorted shape of the signal and measure the elastic waves amplitude in units of mechanical stress (Pa).

It has been established how much of the mechanical energy from the ball collision with the prism surface is consumed to form the elastic wave, wherein the stress in it was registered, which in turn made it possible to calculate the energy in this wave. The test experiment exemplified in Fig. 1, *a* showed that it is possible to correctly record the PFS elastic wave and therefore, to calibrate the PFS, thereby enabling its usage for research in the field. In this case, the PFS was recorded without AR pre-amplification (Fig. 1, *a*). Fig. 1, *b* [19] shows a general view of a unit for recording the elastic waves by means of the photoelasticity method, which was used for such research.

The pulse amplitudes for the fastest low-frequency mode S_0 [18] in the prism are compared and give a sensitivity coefficient $CS_{pf} = 0.78/62.72$ mV/kPa $= 0.01$ mV/kPa within the frequency range 10–30 kHz.

Further, this result was used during calibration of the manufactured well sensor, which was performed as follows. The well AES and the PFS were placed on a concrete unit with the sizes $1000 \times 1000 \times 1000$ mm. At the distance of 100 mm from the place of installation of the sensors the elastic wave was excited by means of a dynamic emitter. Then, the first arrival amplitudes from both sensors were compared and the sensitivity coefficient of the well AES was determined. Both sensors recorded the waves without pre-amplification.

Fig. 2 shows the signals from the well AES (*a*) and the PFS (*b*).

Fig. 3 shows the spectra of these signals. The frequency ranges of these spectra are evaluated by median frequencies of 12 kHz for both sensors.

The sensitivity of the well sensor can be evaluated by applying a previously derived sensitivity coefficient for PFS within the frequency range 10–30 kHz. We obtain

$$CS_{ws} = \frac{PV_w}{PV_{pf}} CS_{pf} = \frac{134.8\,\text{mV}}{0.94\,\text{mV}} 0.01\,\text{mV/kPa} = 1.4\,\text{mV/kPa},$$

where CS_{ws} — the conversion (sensitivity) coefficient of the well sensor, CS_{pf} — the conversion coefficient of the PFS, PV_{ws} and PV_{pf} — the amplitudes of the first arrivals of the well sensor and the PFS, respectively. The sensitivity coefficient derived thereby for the well sensor was 1.4 mV/kPa for the frequency range 10–30 kHz.

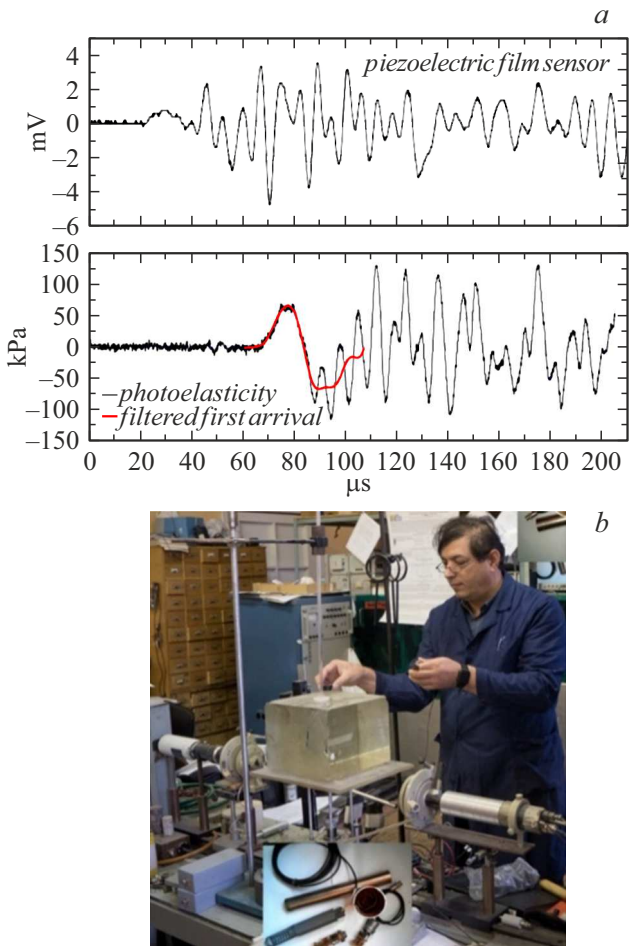

Figure 1. Comparison of the PFS signals with the reference signals obtained when recording by means of the photoelasticity method (*a*). Photograph, the general view of the unit for recording the elastic waves, the photoelasticity method (*b*).

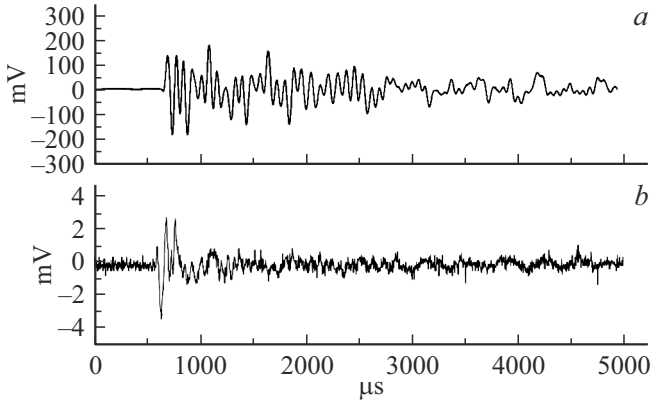

Figure 2. Calibration of the well sensor by means of the reference PFS: the signal recorded by the well AES (*a*); the signal recorded by the PFS (*b*).

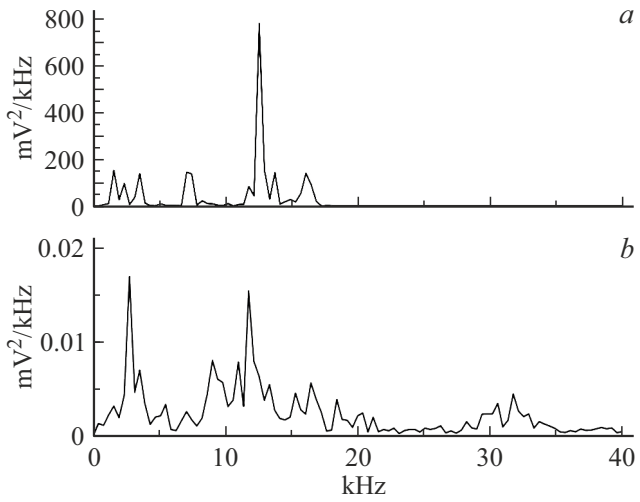

Figure 3. Spectrum of the signal from the well AES (*a*); Spectrum of the signal from the PFS (*b*).

The work [27] provides the measurements of acoustic properties of the concrete reinforcement and the rock massive near one of the wells, in which a standard sensor of the AE underground structures monitoring system is fixed, and analyzes the velocities of propagation of the acoustic waves in the concrete reinforcement.

2. Practical application of the well sensors and analysis of the shapes of signals of the concrete reinforcement and the rock massive in response to impact

The measurements were performed to study the acoustic properties under response of the concrete reinforcement and the rock massive to impact. The impact was provided by the steel ball of the weight of 4.684 kg directly hitting the concrete reinforcement via a steel plate fixed to the concrete reinforcement as well as an embedment inside the concrete wall. The ball was suspended as a pendulum. The massive response was recorded by means of a two-channel digital storage oscilloscope of the ACK type connected to a notebook. The following sensors were used: the channel 1 — the PFS connected to the oscilloscope via the pre-amplifier ($K_{gain} = 400$); the channel 2 — the AES without pre-amplification; the recording was started by means of an external sensor AE 100. The PFS and AES characteristics measured in the laboratory are shown in Fig. 2. The diagram of the measurements in the excavation (well) is shown in Fig. 4. The starting sensor was placed on the concrete reinforcement at the distance of 150 mm to the impact point and the PFS was also placed on the reinforcement at the distance of 400 mm to the impact point. The well AES was placed at the depth of 3000 mm in a horizontal well drilled perpendicular to a plane of the excavation wall. The thickness of the concrete

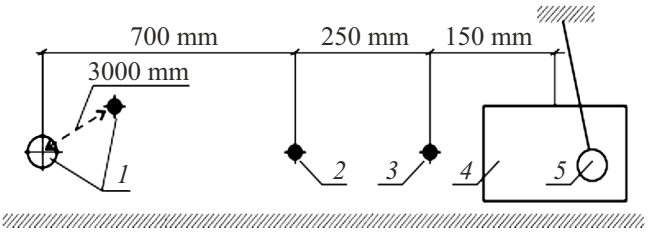

Figure 4. Diagram of the measurements of the rock response to impact excitation by the steel ball directly hitting the concretes reinforcement on the plate fixed to the concrete wall and the embedment inside the rock massive through the concrete. *1* — the well, in which the mine sensor is placed at the depth of 3 m, *2* — the PFS, *3* — the starting sensor, *4* — the impact point (the steel plate or the embedment), *5* — the heavy steel ball.

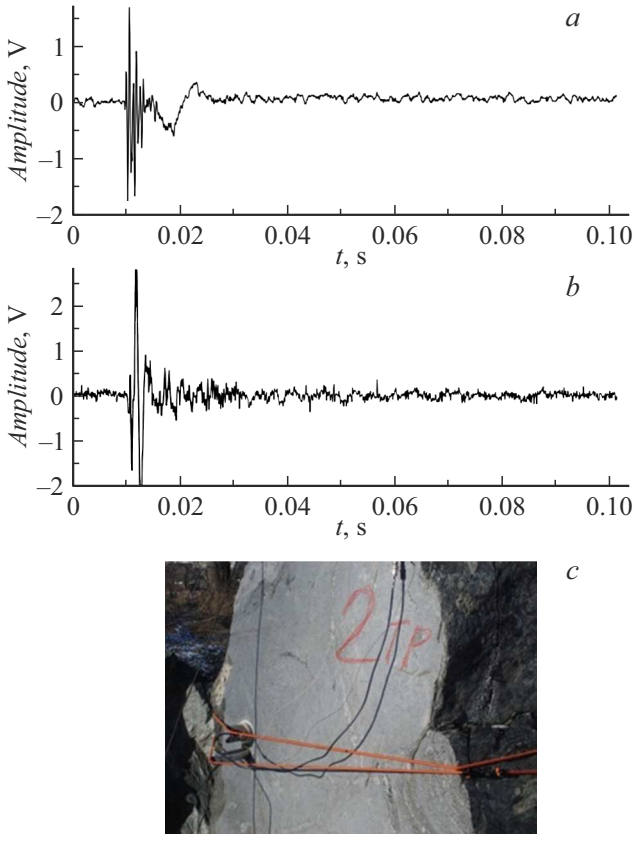

Figure 5. Shapes of the signals of the sensors: *a* — placed on the concrete embedment; *b* — inside the well in the rock massive at the distance of 3200 mm to the ball impact as well as the sample (photograph) of the rock massive formed by the biotite gneisses (*c*).

reinforcement — 1500 mm. Thus, the well sensor was exactly inside the rock massive. The distance of the well to the impact point was 1100 mm. The monitored rock massive is formed by biotite gneisses (Fig. 5, *c*).

Fig. 5 shows typical signals recorded by the PFS fixed directly to the concrete wall of the excavation (Fig. 5, *a*) and by the AES placed in the well at the depth of 3000 mm

inside the massive (Fig. 5, *b*). The impact was through the steel plate fixed to the concrete wall.

3. Analysis of the shapes of the response signals

Fig. 6 shows a cross-spectrum and a correlation function of response from two successive impacts of the same energy: as recorded by the PFS (Fig. 6, *a*); as recorded by the well (the red AES) sensor inside the well (Fig. 6, *b*).

It is clear from Fig. 6a that when the elastic wave is excited by ball impact on the plate fixed on the concrete reinforcement the acoustic energy, the PFS (black), is concentrated in two frequency ranges — around 0.2 kHz and around 1.5 kHz. The energy recorded by the well sensor, the AES (red), inside the rock massive is accumulated around 0.5 kHz (Fig. 6, *b*).

Fig. 7 shows a cross-spectrum and a correlation function of response from two successive impacts of the same energy when hitting the embedded reinforcement that passes through concrete into the massive: as recorded by the PFS (Fig. 7, *a*); as recorded by the AES inside the well (Fig. 7, *b*).

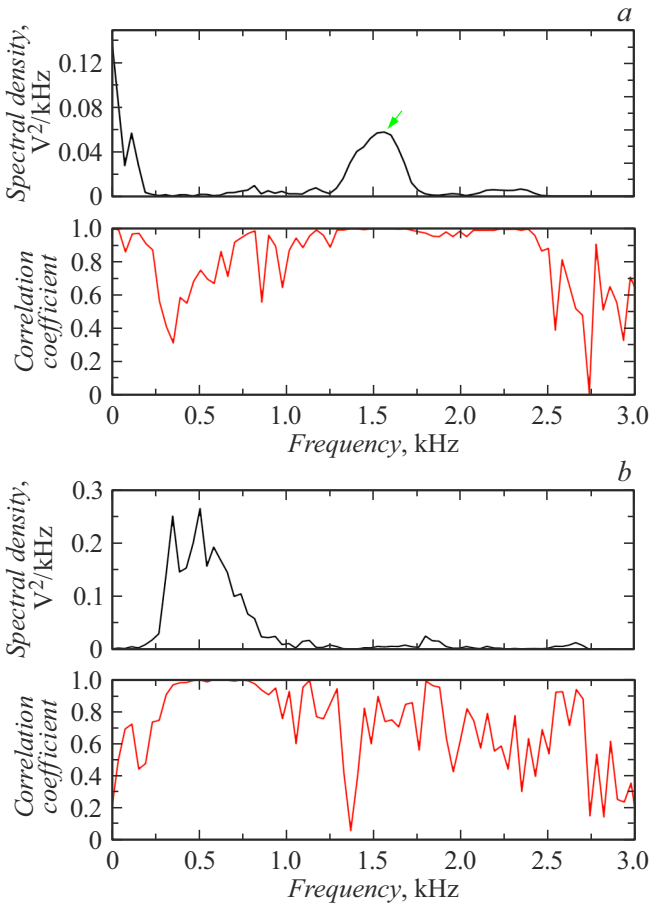

Figure 6. Cross-spectrum and the correlation function of the signals from two successive impacts of the same energy on the plate: as recorded by the PFS (*a*); as recorded by the AES inside the well (*b*).

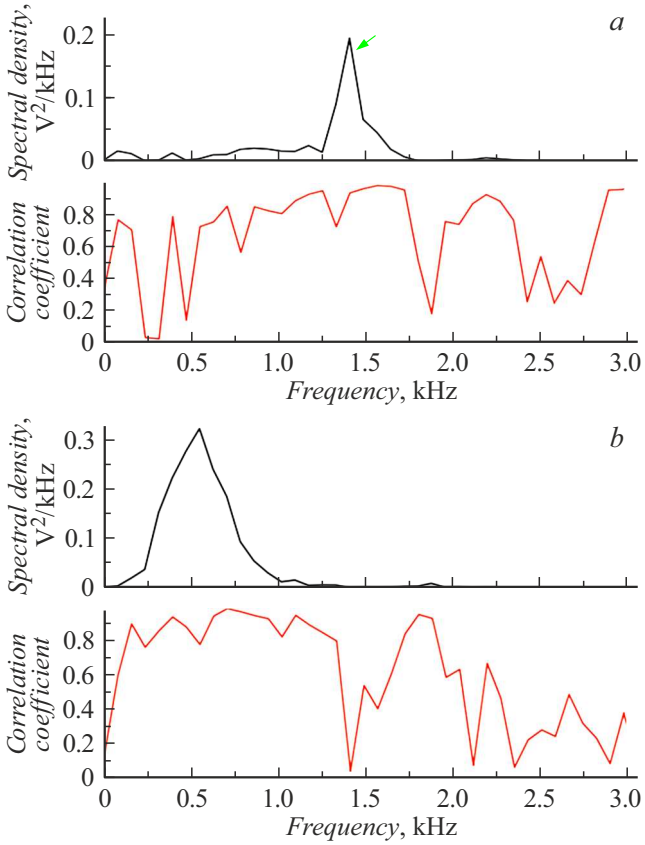

Figure 7. Cross-spectrum and the correlation function of the signals from two successive impacts of the same energy on the embedment: as recorded by the PFS (*a*); as recorded by the AES inside the well (*b*).

It should be noted that the spectrum (Fig. 7, *a*) and the shape of the signal (Fig. 5, *a*) when hitting the embedded reinforcement differ from the spectrum and the shape of the signal when hitting the plate (Fig. 6, *a* and *b*, respectively) with the PFS by the fact that hitting the embedment includes recording only a high-frequency component of response of the concrete reinforcement around 1.5 kHz. Accordingly, in this case the response spectrum is represented only by one frequency range (Fig. 7, *a*) unlike the spectrum of hitting the plate (Fig. 6, *a*), where the impact energy is distributed in two frequency ranges. The massive responses recorded by the well AES for the two cases of excitation (Fig. 6, *b* and 7, *b*) are almost the same in terms of a frequency composition — the elastic waves energy is accumulated around 0.5 kHz. Fig. 8 shows the cross-spectrum and the correlation functions of such signals from the two successive impacts of the same energy on the excavation wall without the concrete reinforcement.

It is clear that the signal and its spectrum are represented by a monochromatic process at the frequency of 0.8 kHz and the Q factor of this process in this cases is higher than for the case of recording the response of the rock

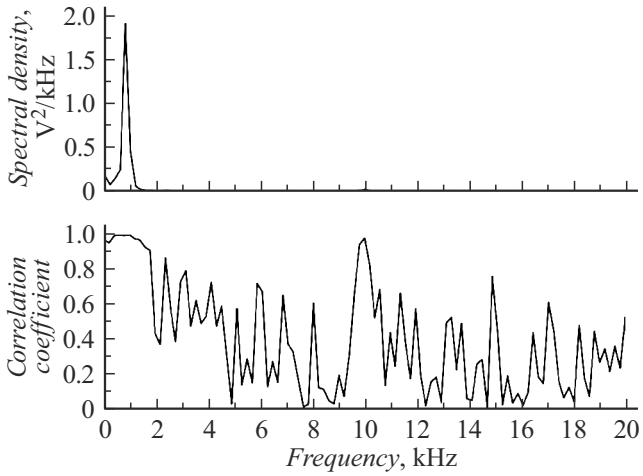

Figure 8. Cross-spectrum and the correlation function of the signals from two successive impacts of the same energy on the wall of the massive without the concrete reinforcement as recorded by the mine sensor in the well.

massive in the excavation strengthened by the concrete reinforcement (Fig. 6, *b*). Since the maximum amplitudes of the processes from the DAE are approximately equal (around 2–3 V) for the two cases of the measurements (Fig. 6, *b*), we deduce that contact conditions of the sensor with the rock are comparable for both the cases. The increased frequency of response of the massive without the concrete reinforcement (0.8 kHz) as compared with the first case of the measurements (0.5 kHz) and the increased Q factor of response of the rock massive may indicate lesser fracturing of the rock massive in the new excavation without the concrete reinforcement. It should be noted that the correlation function reveals another significant peak at the frequency around 10 kHz (Fig. 8). As it is clear from Fig. 8, the energy of oscillations at this frequency is insignificant as compared to a fundamental frequency of the process (0.8 kHz).

Supposedly, this peak may refer to a low-frequency part of natural oscillations of the AES.

4. Discussion of the results

The calibration of the well sensors and determination of their frequency responses in the laboratory and the field enabled more exact pre-measurement of the velocity field for propagation of the elastic waves in the rock in the region of sensor installation in the well. The velocity of elastic wave propagation oscillated around 5318 m/s, which is almost the same as the calculated velocity [18]. In order to measure the energy of the AR source in the absolute unit scale (J) for the recorded acoustic pulses, the energy balance „AR source–transmitting medium–AR receiver" has been analyzed in the laboratory using the spectral analyzer. The experiment included measurement of a portion of mechanical energy spent for excitation of the elastic wave and independent measurement of stress in the elastic wave, which was taken to calculate the wave energy. The wave radiation source was elastic collision of the steel ball (AR source) with the surface of the glass prism $190 \times 240 \times 240$ mm (transmitting medium) and the stresses in the elastic wave were measured by the photoelasticity methods (AR receiver) [19,28].

The two independent methods for determination of elastic interaction energy were compared to show discrepancy between the results below 20 %. I.e., for the model case almost the entire energy of elastic collision passed into energy of elastic oscillations of the prism, which in turn has an almost perfect transfer function. The spectral composition of the interaction energy was also determined [29].

To adapt this procedure to the underground structure, a piezoelectric receiver with a linear frequency response in the range up to 30 kHz [18] was developed, manufactured and calibrated to measure the elastic wave stresses. It was placed in the underground structure in the region of one of the wells which stationarily include standard AESes of the AE monitoring system. The sensor was used to measure the spectral composition of the rock massive response to massive excitation by the impact of the ball with weight of $M = 4.684$ kg, and also energy of the elastic wave formed from the impact by the ball was estimated.

Comparison of the estimate of the elastic energy (about 0.3 J) with the loss of mechanical energy upon impact by the ball (about 6 J) is very approximate [18]. This is first of all due to the fact that when the elastic wave is excited by a ball hitting the excavation surface, the collision is not purely elastic, but is accompanied by rock destruction at the point of contact, to which a significant portion of the mechanical energy of the ball lost during the collision is used. Secondly, it is due to the fact that the medium transfer function is unknown and it can be determined after exclusion of the first reason of discrepancy between the results. Therefore, in order to correctly evaluate the energy, it is necessary to eliminate the massive destruction when it is excited by the ball impact, for example, by installing embedded parts. The spectral density of massive excitation due to the ball impact is concentrated within the range 0.7–3.2 kHz [28].

Conclusion

The created algorithm can diagnose separately all the AE monitoring lines during operation of the AE monitoring system and it was demonstrated that the well AESes with specified characteristics could be used in conditions of the real rock massive with concrete reinforcement. A channel is created for transfer of data of the AE monitoring system from the standard computer to any other computer (for example, notebook) for further independent AR analysis in the field and in the laboratory. An algorithm for use of the broadband piezoelectric transmitters was developed, so was a capability of their calibration in the laboratory and in the field. It was made possible only after creating

a mobile device that is usable both in the laboratory and in the field. It also included development of methods of optimization and recording AES frequency responses in the field. It is recommended to use the algorithm when controlling operation of the signal recording lines and calibrating them by the AE automated monitoring system, especially, when there is no location of the signal sources during AE control of the object. The developed algorithm provides valuable data on the current state of the object and specifies a procedure and scope of necessary recorded parameters of the AE signals during acoustic emission monitoring of elements of underground structures of a hazardous production facility in order to evaluate their geomechanical stability and safe operation, thereby detecting potential problems with substantially reducing a calculation error.

The defining parameters to be used for determining a technical condition shall be selected based on results of analyzing a database of the AE monitoring of the underground structures and periodically determining the velocity field for propagation of the elastic waves in the controlled rock massive, and of expert examination.

Conflict of interest

The authors declare that they have no conflict of interest.

References

[1] A.A. Reshetov, A.K. Arakelyan. *Nerazrushayuschii kontrol i tekhnicheskaya diagnosktika energeticheskikh objectov* (Chuvashskii un-t, Cheboksary, 2010) (in Russian)

[2] V.I. Ivanov, V.A. Barat, *Akustiko-emissionnaya diagnostika* (Spektr, M., 2017). (in Russian)

[3] A.A. Aksenov, I.A. Ozhiganov, O.A. Isyanov. Gorny zhurn, (in Russian) **9**, 83 (2014).

[4] E.N. Sher, N.I. Alexandrova, M.V. Aizenberg-Stepanenko, A.G. Chernikov. J. Min. Sci., **43** (6), 20 (2007).

[5] A.M. Molodets, V.V. Avdonin, A.N. Zhukov, Yu.M. Shulga. Deformation and Destruction of Mater., **9**, 2 (2008).

[6] A.V. Popov, A.B. Komlev, D.N. Teslya. Kontrol. Diagnostika, (in Russian) **8** (242), 32 (2018).

[7] G. Su, V. Gang, S. Chai, G. Zhao. J. Central Southern Univ., **27** (10), 2883 (2020). DOI: 10.1007/s11771-020-4516-6

[8] T.V. Popova, A.E. Mayer, K.V. Khishchenko. J. Phys.: Conf. Ser., **653**, 012045 (2015).

[9] K.W. Liu, W. Yuan, Y. Yan, X. Wang. Symmetry, **11** (8), 1040 (2019). DOI: 10.3390/sym11081040

[10] D.A. Mengel. Gorny informatsionno-analiticheskiy byulleten (nauchno-technichekii zhurn.), **3**−**1**, 149 (2020). (in Russian) DOI: 10.25018/0236-1493-2020-31-0-149-160

[11] V.S. Kuksenko, Kh.F. Makhmudov, B. Ts. Manzhikov. Fiziko-tekhnicheskie problemy razrabotki poleznykh iskopaemykh, **4**, 29 (2010). (in Russian)

[12] M.G. Potanina, V. Smirnov, A. Ponomarev, P. Bernar, A.A. Lyubushin, Sh.P. Shoziev. Fizika Zemli, **2**, 126 (2015). (in Russian)

[13] S. Stanchits, J. Burghardt, A. Surdi. Rock Mech. Rock. Eng., **48**, 2513 (2015).

[14] M.D. Ilinov, D.N. Petrov, D.A. Karmanskii, A.A. Selikhov. Gornye nauki i tekhnologii **8**, *4*, 290 (2023). (in Russian) DOI: 10.17073/2500-0632-2023-09-150

[15] C.G. Lacidogna, N. Pugno. *Proc. X Conf. Sound and Vibration* (Stockholm, 7−10 July, 2003)

[16] V.V. Nosov. Defektoskopiya **12**, 24 (2014). (in Russian)

[17] V.S. Kuksenko, N.G. Tomilin, Kh.F. Makhmudov, A.V. Benin. Tech. Phys. Lett., **33** (1), 62 (2007). DOI: 10.1134/S1063785007010178]

[18] V.N. Saveliev, Kh.F. Makhmudov. ZhTF, **90** (1), 143 (2020). (in Russian) DOI: 10.21883/JTF.2020.01.48676.74-19

[19] V.A. Petrov, V.A. Pikulin, A.O. Rozanov, V.N. Saveliev, S.A. Stanchits. *Sposob opredeleniya energii signala akusticheskoi emissii v tverdom tele* (Patent Rossiiskoi Federatsii № 2037821, 1995) (in Russian)

[20] S.P. Bykov, K.A. Kuznetsov, A.V. Yushin, I.N. Skryabikov. *Sposob opredeleniya rasstoyaniya mezhdu preobrazovatelem i istochnikom akusticheskoi emissii* (Patent № 2397490 C2 Rossiiskaya Federatsiya, MPK G01N 29/14. Zayavitel OAO „IrkutskNIIchimmash")

[21] S.A. Bekher, T.V. Sych. Diagnostics, Resource and Mechanics of Materials and Structures, **2**, 14 (2016). DOI: 10.17804/2410-9908.2016.2.014-020

[22] *Trebovaniya k preobrazovatelyam akusticheskoi emissii, primenyaemym dlya kontrolya opasnykh proizvodstvennykh objektov* (RD 03-300-99. 01.10.1999, 1999) (in Russian)

[23] A.Yu. Iskra, I.Yu. Rasskazov, G.A. Kalinov, Yu.I. Bolotin. Gorny zhurn., **6**, 72 (2006). (in Russian)

[24] G.A. Kalinov, I.Yu. Rasskazov, A.Yu. Iskra, D.A. Kulikov, K.O. Kharitonov. *Fizicheskaya akustika. Rasprostranenie i difraktsiya voln. Geoakustika*: Sb. tr. XVI sessii Rossiiskogo akusticheskogo obshchestva (GEOS, M., 2005), V. 1, P. 351–354. (in Russian)

[25] A.Yu. Iskra, I.Yu. Rasskazov. Gorny zhurn., **1**, 85 (2007). (in Russian)

[26] K.N. Trubetskoi, D.M. Bronnikov, S.V. Kuznetsov, V.A. Trofimov. Fizika Zemli, **7**−**8**, 78 (1994). (in Russian)

[27] Kh.F. Makhmudov. ZhTF, **92** (12), 1869 (2022). (in Russian) DOI: 10.21883/0000000000

[28] X.F. Makhmudov, V.N. Saveliev, D.V. Saveliev, V.N. Medvedev, S.Yu. Kruglov. *XXIII Peterburgskie chteniya po problemam prochnosti, posvyashchennye 100-letiyu FTI im A.F. Ioffe i 110-letiyu so dnya rozhdeniya chl.-korr. AN SSSR A.V. Sptepanova* (Sankt-Peterburg, Rossiya, 10−12 aprelya 2018), P. 136–37. (in Russian)

[29] I.P. Shcherbakov, H.F. Makhmudov, A.E. Chmel. ZhTF, **94** (1), (in Russian) 48 (2024). DOI: 10.61011/JTF.2024.01.56900.86-23

Translated by M.Shevelev